Dearborn, Michigan
NOISE-CON 2008
2008 July 28-30

Characterization and active reduction of operating noise of a diesel generator

Cory Papenfuss[a]
Tom-Davy W. Saux[b]
Chris R. Fuller
Marcel C. Remillieux
Vibrations and Acoustics Laboratories, Mechanical Engineering Dept.
Virginia Polytechnic Institute and State University
Blacksburg, VA 24060

ABSTRACT

This paper discusses the methodology and results of a noise audit and active control testing on a portable single-cylinder diesel generator. Using a large microphone array, a spectral intensity map of all external surfaces of the generator set was constructed from experimental measurements. Two primary noise sources were measured; a relatively directional high-frequency structurally-coupled engine component, and low-frequency fundamental exhaust firing-order harmonics. The high-frequency was treated passively. The low-frequencies were reduced using the feed-forward Filtered-X LMS with a reference derived directly from the electrical generator coupled to the diesel engine. A custom analog circuit was designed and constructed to generate phase-locked integer-multiples of the subharmonic of the machine's electrical frequency corresponding to the firing pulses. This provided very high coherency for the active noise control with commensurate reduction performance.

1. INTRODUCTION

Portable generators are a necessity for many industrial, personal, and military applications. Unfortunately, using an internal combustion engine to generate electricity produces unwanted noise in addition to the desired electrical power. Reduction of the noise produced by these machines is often done as an afterthought to the original design. For the investigation of this paper, a noise audit and active/passive treatment was performed on a 3-kW single-cylinder diesel generator. The generator set already had noise treatments applied by encasing it in an aluminum enclosure, with passive poro elastic treatments on the panels and on all inlets and outlets. In order to improve the noise reduction, a combination of additional passive treatment and active noise control (ANC) using an adaptive feed-forward algorithm was implemented and its performance measured. The generator with a representative active control source to demonstrate the potential of ANC can be seen in Figure 1.

[a] Email address: papenfuss@vt.edu
[b] Email address: tomdavy@vt.edu

Figure 1: Photograph of 3kW generator with example prototype ANC source.

2. NOISE SOURCE AUDIT AND TREATMENT

A. High Frequency Measurement Procedure

The microphone phased array shown in Figure 2 was used to map the generator enclosure radiation noise sources. The array had a star configuration consisting of seven arms with nine microphones per arm. The inside and outside diameters of the array were 9.8 inches and 59.8 inches, respectively. The array center body was provided with a laser pointer that projects a laser dot along a line perpendicular to the array plane passing through the center of the array. This laser pointer was used for alignment purposes.

Phased-array measurements were carried out from four positions relative to the generator. The array was successively placed at 128 inches from each side panel of the generator such that the laser was pointing to the center of the top edge of the panel.

Figure 2: Photograph of the 63-element microphone phased-array.

The 63 microphone signals were sampled simultaneously at 51,200 samples per second in 25 separate blocks of 16,384 samples each. Time-domain data was processed using a frequency-

domain, phased-array, beamforming code developed at Virginia Tech. Diagonal removal was used in the post-processing of the phased-array data to minimize the effects of uncorrelated background noise. For each array position, the data was processed over a scanning plane that contained the panel the array was facing, with a 1-inch resolution in both horizontal and vertical directions. Results were obtained in the form of narrow-band acoustic maps in the range of 1200 to 1500 Hz. The four side panels measured by the array are labeled as in Table 1.

Table 1: Panels measured by the array.

Face 1:	Operator panel	27” x 26” (W x H)
Face 2:	Access panel	34” x 26”
Face 3:	Opposite operator panel	27” x 26”
Face 4:	Exhaust panel	34” x 26”

B. High Frequency Results

Figure 3 shows the average microphone spectrum for the array positioned in front of face 2. This figure helped to identify specifying frequency ranges to choose for plotting the beamforming maps. For example, the figure indicates that a large part of the high-frequency spectral energy is contained in the frequency range of 1200 - 1500 Hz, with a dominant peak around 1400 Hz. This frequency band was chosen to identify the noise sources on the side-panel surfaces.

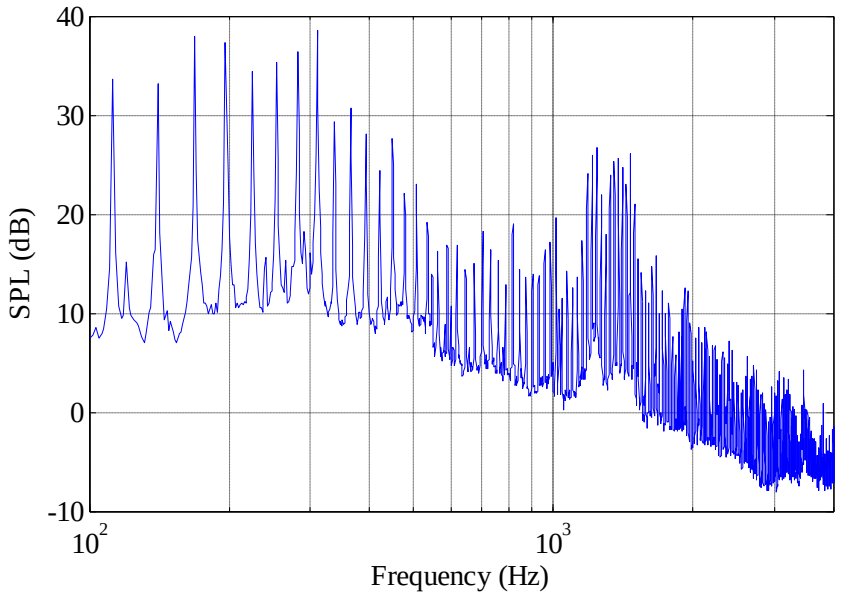

Figure 3: Average microphone spectrum for the array in front of face 2.

Figures 4a-4d show the beamforming maps of the generator noise for the array positioned in front of faces 1 to 4, respectively. The sound pressure level (SPL) in these plots is uncalibrated, but this is unimportant as only the relative sound levels are necessary to identify the noise sources.

In Figure 4a (face 1), a strong radiation component is observed below the generator enclosure, which can be explained by the presence of drainage holes on the bottom pan of the structure. The bottom pan is not resting directly on the ground, but is lifted by about 4 inches due to the presence of forklift skids. Noise radiating from these holes thus reflects off the ground and

contributes largely to the 1400 Hz tones. Figure 4c shows similar results for the opposite panel (face 3)

In Figure 4b (face2), most of the noise is emitted from the top of the enclosure, where the fan exhaust, the fan intake and the engine exhaust are located. These sources, together with the radiation of the top panel, are likely causes of the sound pattern observed.

In Figure 4d (face 4), the major contribution is located in the left half of the panel surface, indicating that this particular part of the structure is radiating considerably within the frequency range of interest. The engine muffler is behind this panel and is likely exciting it acoustically from within.

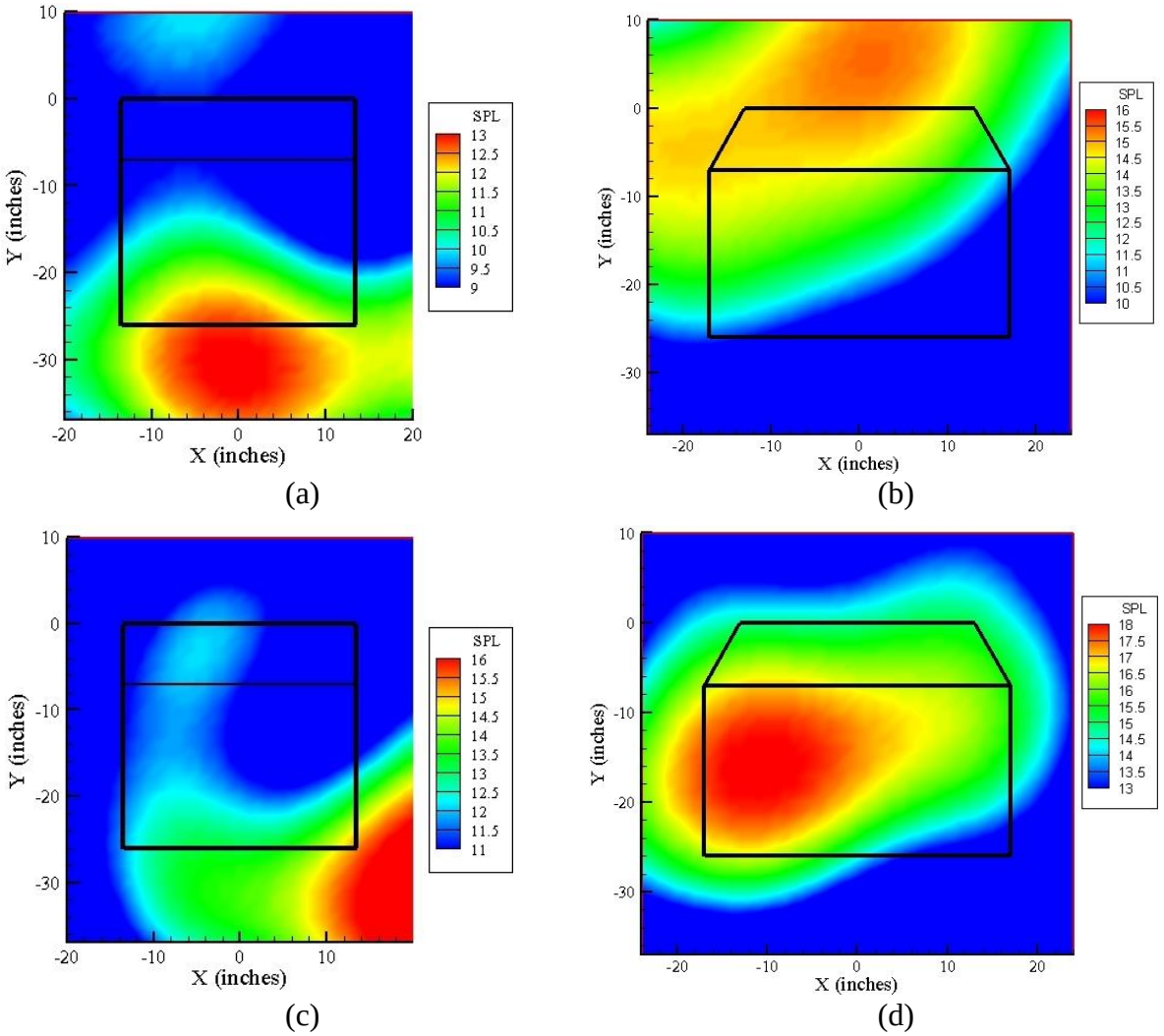

Figure 4: beamforming maps of (a) face 1 at 1394 Hz, (b) face2 at 1380 Hz, (c) face 3 at 1411 Hz and (d) face 4 at 1412 Hz. The shape of the compressor is outlined in black solid line.

Several parts of the enclosure are contributing to the 1400 Hz tones, by emitting both structure-borne and air-borne noise. However, the dominant SPL zones on Figure 4 are just a few decibels above the average SPL. Thus, even if the dominant sources are eliminated, secondary sources will still add up to produce significant acoustic power. Therefore, an effective passive noise control strategy has to both reduce local dominant sources and provide a global treatment.

Based on these considerations and on the observations made from the beamforming maps, the following additional passive noise control treatments were added to the enclosure:

(i) Ribs made of ½ inch angle aluminum were attached to face 3 and face 4, in order to add stiffness locally. This would reduce the 1400Hz radiation shown prominently in Figures 4c and 4d.

(ii) The absorptive materials from the air inlet and outlet ducts on face 3 was removed, replaced and repositioned for better noise control. The standard material was also augmented with additional absorptive material. Care was taken to keep the cross sectional areas of the inlet and outlet duct the same size, in order to maintain the same air cooling flow.

(iii) Absorptive material was added to the inside of the enclosure particularly on the operator panel side. Care was taken to add a minimum of material and not impede access or operation/cooling of mechanical components.

(iv) Acoustic material was located in the skid access slots under the machine on the region of the drainage holes discussed above. This treatment was not meant to be practical but to assess how much sound energy was leaking out of these drainage holes.

The performance of these passive noise control strategies is described in section 4.

C. Low Frequency Coherence Measurement

In addition to the phased-array maps, the coherence between the far-field sound levels to both structural and acoustic sources was measured. An accelerometer was placed on the cylinder head of the diesel engine and the coherence between it and a far-field microphone was measured as in Figure 5. As can be seen, a number of harmonics below 400 Hz show reasonably good coherence, which would allow for good active noise control.

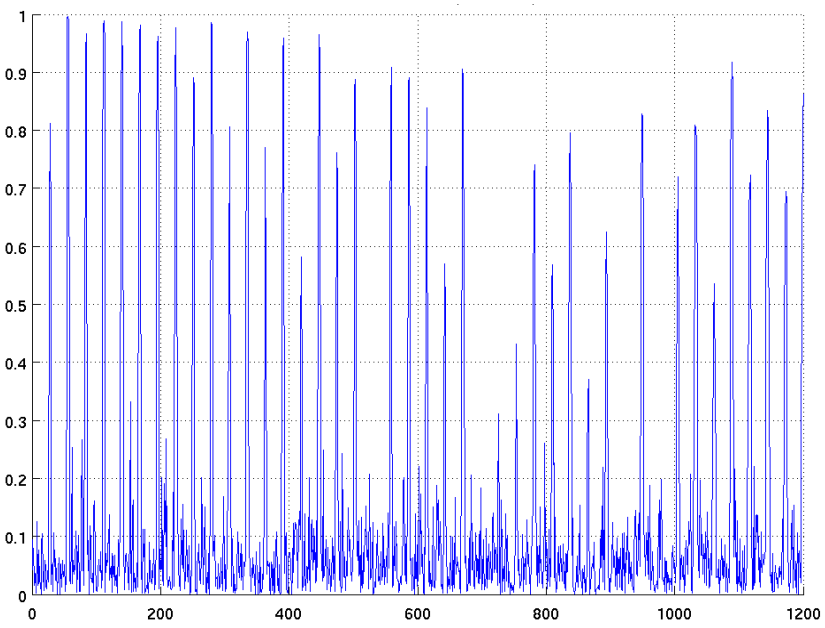

Figure 5: Coherence between far field microphone and accelerometer on cylinder head.

Together with structurally-borne sound, the exhaust pulsations were a likely contributor to far-field, low-frequency sound. A microphone was placed very near the exhaust, but not within the hot exhaust gas stream. The coherence of this acoustic signal to the far-field microphone can be seen in Figure 6. Almost all harmonics up to 500 Hz have coherency above 0.95, with most greater than 0.99. This implies the bulk of the far-field low-frequency (<500Hz) noise comes from the combustion events and their harmonics. This would be exploited by the reference circuit construction of Section 3.

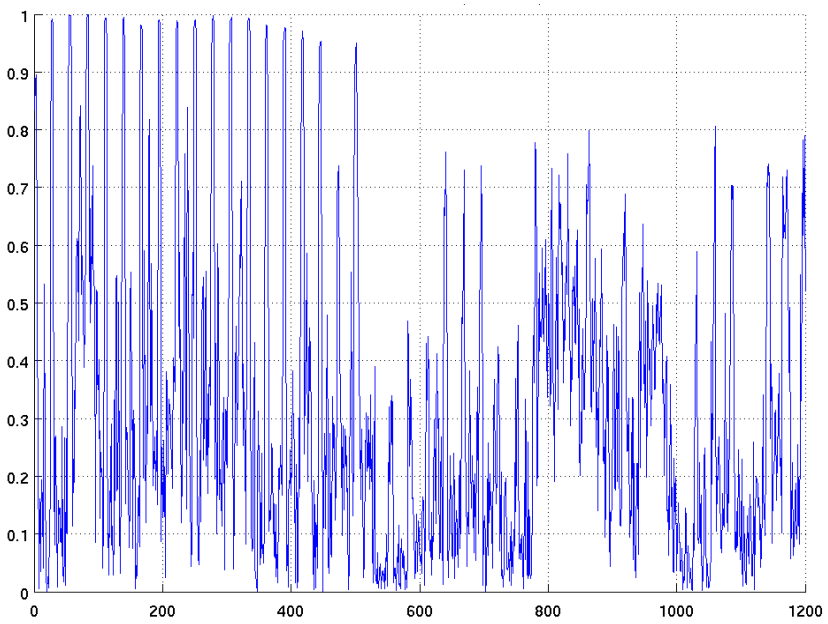

Figure 6: Coherence between far field microphone and microphone located near exhaust outlet.

3. ACTIVE CONTROL DESIGN

The active control algorithm chosen was the well-known Filtered-X Least-Mean Squares, or FxLMS. This has been widely studied[1-2] and has very good performance when reference signal coherent with the noise is present. The noise audit of Section 2 showed that the low frequency noise primarily came from the exhaust, indicating that it was mostly likely caused by the combustion cycles. Typically for this type of problem, an accelerometer is placed on the engine for a reference for the feed-forward control, but attaining good coherence by this manner is often problematic. The coherence investigation of Section 2 implies a microphone near the exhaust would be a good reference. Unfortunately, this has the problem of not only being in close proximity to the hot exhaust gases, but also provides a feedback path for the control. While this can be compensated for in the control design, performance and robustness often suffers. Rather, for this investigation, a dedicated hybrid analog/digital circuit was designed and constructed to produce a fully decoupled, yet highly coherent reference signal.

A. Reference Generation

The electrical side of the generator used for this experimental setup consisted of a synchronous permanent magnet machine coupled to a dedicated full-time inverter. This configuration allows for decoupling of the engine speed to the required synchronous electrical frequency of either 60 Hz or 400 Hz. It also allows for a high-efficiency permanent magnet machine to be used without

requiring field adjustment for maintaining the correct output voltage. In addition to the main windings, the machine also had a small, lower-voltage single-phase winding used to charge the engine's starting battery. This winding provided the necessary phase-locked reference to the engine rotation at a lower voltage than using one of the main windings.

Although the auxiliary winding of the synchronous machine provided an accurate phase reference to the engine, it was at a higher frequency than the fundamental firing order harmonic. The electrical frequency of the winding is given by the following relationship:

$$f = \frac{RPM \times Npoles}{120} \tag{1}$$

However, the 4-cycle engine only fires every 720 degrees of rotation. From the number of poles on the machine, the integer ratio between the firing of the machine and the electrical frequency was calculated.

The circuit used to generate the phase-locked reference is shown in Figure 7. The prefilter provided voltage reduction and filtering any harmonics higher than the fundamental electrical frequency. The zero-crossing detector generated a pulse at this frequency, which was reduced by the integer ratio, and used to generate a saw tooth at the lower frequency. Since a saw tooth waveform has both even and odd harmonics, all frequency multiples of the firing pulse were generated in the reference circuit.

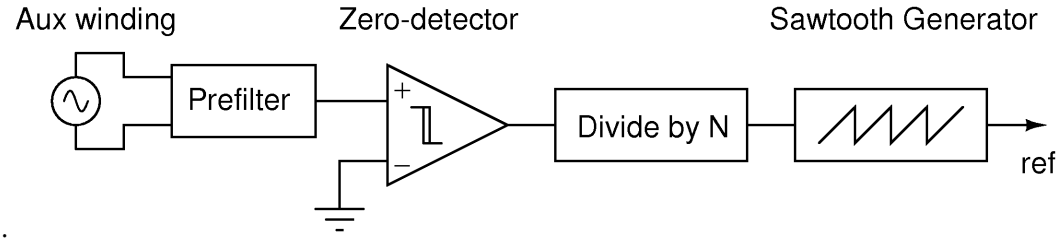

Figure 7: Pseudo-schematic of reference generation circuit.

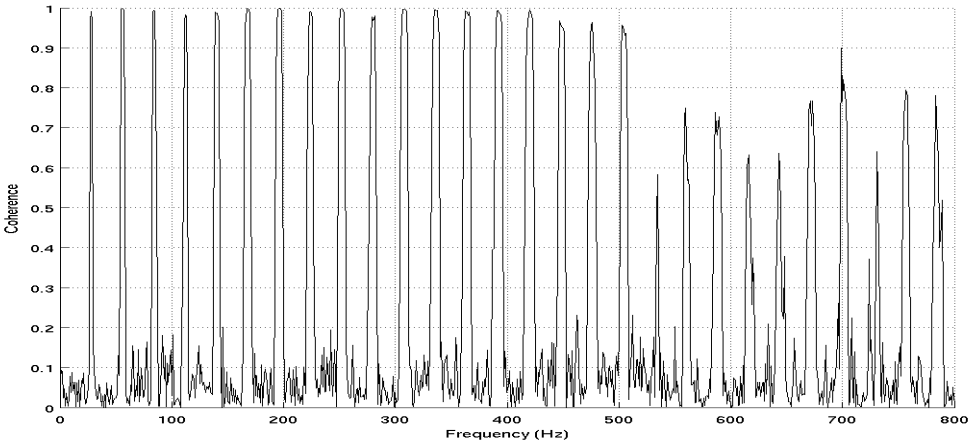

Figure 8: Measured coherence between reference signal and far field microphone.

The performance of the reference circuit can be seen in the coherence plot of Figure 8. This data was taken on the actual machine in operation and shows near unity coherence from all harmonic through approximately 500 Hz. That corresponds to the first 20 firing-order harmonics of the diesel engine.

B. Controller Design

The FxLMS controller used was constrained to specific control bandwidths in order to limit the amount of power required to drive the source speaker. The speaker chosen was an off-the-shelf 10" subwoofer. The primary contributions to the total A-weighted SPL coming from the machine were grouped primarily in a band from 50-500 Hz, and another from approximately 1100-1500 Hz. This can be seen in the "control off" plots of Figure 9. The contributions from 1100-1500 Hz were well within the frequency range of using passive treatment, so only the range less than 500 Hz was chosen for the active control bandwidth. The 0-500 Hz control bandwidth included a large tone at approximately 56 Hz, which required a significant amount of actuator authority and amplifier power to drive. Because of this, a 100-500 Hz bandwidth was also investigated in order to reduce the actuator requirements with a minimal loss of overall global A-weighted reduction.

Using the reference circuit from Section 3A, the FxLMS algorithm was implemented in a PC with dedicated real-time data acquisition boards and a DSP coprocessor card. Analog filters were configured on the reference, error, and output channels to limit the control bandwidth. A total of 256 coefficients were used with a sample rate of 4096 Hz. For most of the tests, a Single-Input, Single-Output control configuration was used.

4. PERFORMANCE

The purpose of these reported tests was to demonstrate the potential of ANC for low frequency noise reduction. Thus the active speaker arrangement of Figure 1 was used. Future work will consider integrating the active speaker into the enclosure structure. The performance of the passive and active treatments was measured on the generator via a microphone located on each of its four sides at a distance of 3m from the machine center. The generator was run outside in a semi-reverberant location. The microphone near the operator panel was chosen as the error microphone for the active control.

The performance of the 0-500 Hz bandwidth active control at the error microphone can be seen in Figure 9. The black and red lines show the narrowband spectrum of the error microphone with and without the active control running. The blue and magenta lines show a cumulative integral of the same data. The cumulative integral indicates the overall sound level summed from 0 Hz to the frequency of interest. The total broadband performance is the difference between the two curves at the maximum plotted frequency. What this shows is that although the harmonics between 0-500 Hz are reduced between 15-30 dB, after the remaining spectrum from 500-2000 Hz is added, the aggregate reduction is only 3-4 dB. This shows the need to include the passive treatment. The overall reduction is limited by the set of tones centered on 1400Hz.

For the advanced passive control, two different configurations were studied. The first consisted of stiffeners on acoustically "hot" panels and additional poro elastic located in the housing interior. The second considered an addition of absorbing material to areas located just below drainage holes on the bottom of the machine casing. Figure 10 shows the operator side microphone baseline (untreated) case, as well as the two passive cases (active off) and two cases of the aforementioned passive treatment with active control turned on. A significant reduction in radiated sound level can be seen in the 700-3000 Hz frequency bands with the addition of the absorbing material on the bottom of the unit near the drainage holes indicating that they leaked significant sound energy at higher frequencies. In addition, the active control can be seen from Figure 10 to provide significant reduction in the targeted band of either 0-500 Hz or 100-500 Hz.

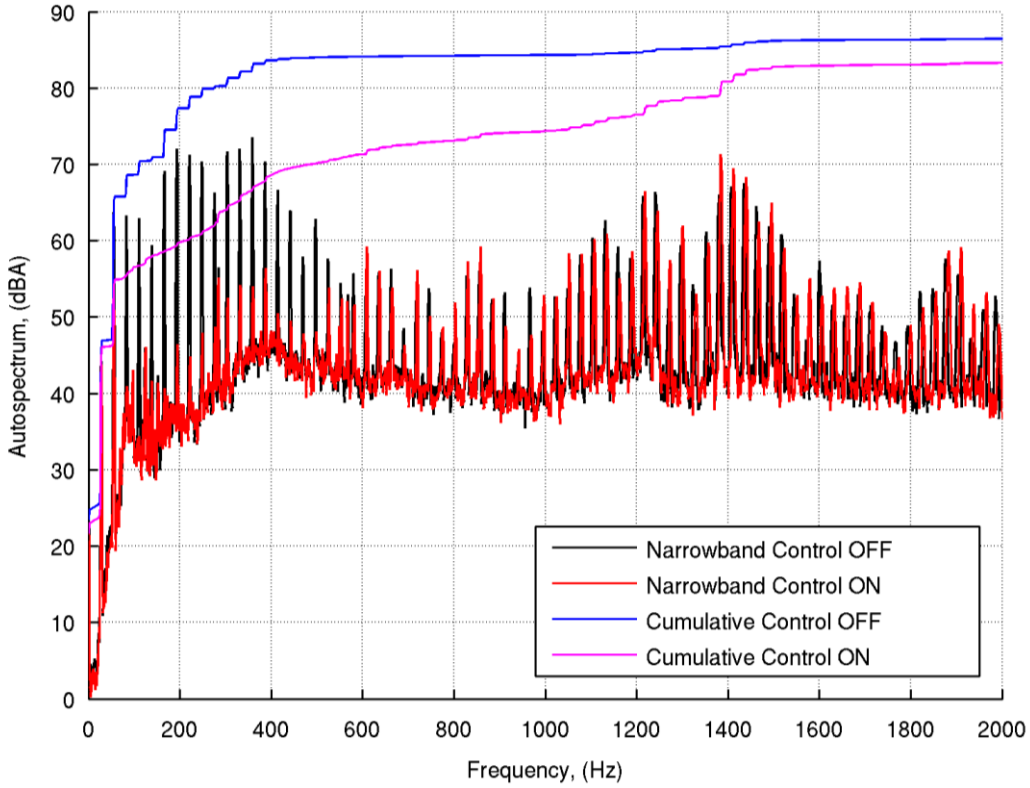

Figure 9: Narrowband and cumulative integral spectral plot of error signal with and without active control.

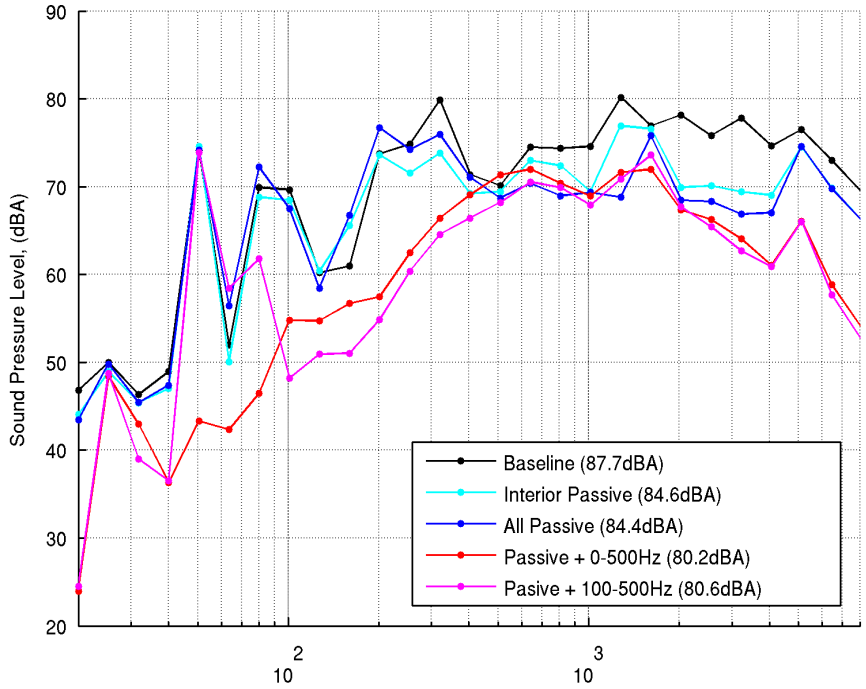

Figure 10: Treatment and active control performance (error microphone in 1/3rd octave bands).

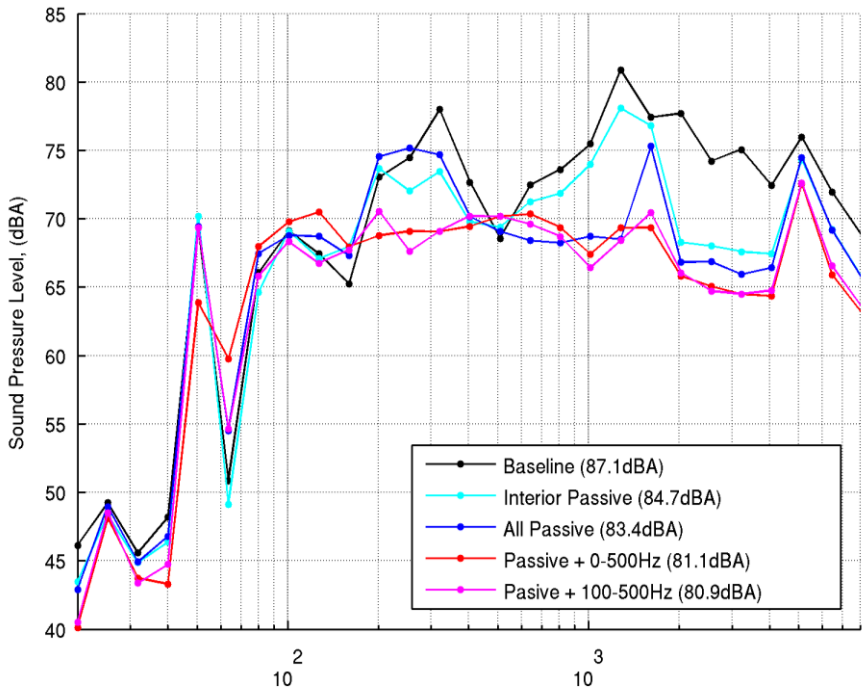

Figure 11: Treatment and active control performance (mean of four monitor microphones in 1/3rd octave bands).

Figure 11 shows the performance at all four microphone locations summed together to give an indication of global sound radiation from the machine. The figure shows very good global reduction of the high-frequencies, while still providing good global reductions for the low-frequencies due to the active source.

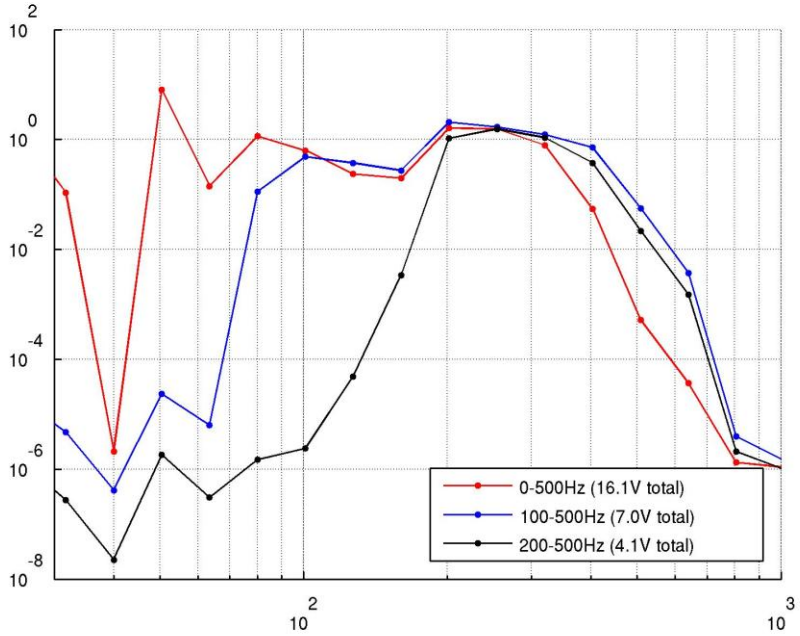

Figure 12: Speaker voltage filtered in 1/3rd octave bands.

Finally, an indicator of how much electrical power was required to drive the active source with different control bandwidths can be seen in Figure 12. The nominal speaker impedance was 2 Ohms, so the approximate power requirements range from 8 W for a 200-500 Hz control bandwidth to 130 W for the 0-500 Hz bandwidth. The perception of the control effect as judged by several listeners indicated little difference in perceived reduction between the 100-500Hz bandwidth and the 0-500Hz bandwidth. In essence, even though the radiated sound levels (A-weighted) at 56Hz are relatively small, they still do contribute to the control cost function, particularly when the cost function has been attenuated more than 10dB or so. Since the required volume velocity to generate a 56Hz tone is much larger than the higher frequencies above 100Hz, the control signal contains very large voltage levels at 56Hz in order to reduce these small components. Thus inclusion of the 56Hz tone in the control bandwidth was judged unnecessary, particularly as it would dictate use of a larger control speaker and loss of generator electrical power and thus reduced efficiency (the ANC system will ultimately be powered by the generator set).

5. CONCLUSIONS

This paper describes the full scale implementation of passive and active noise control on a portable diesel generator. Although the unit was already designed with sound reduction in mind, a noise audit using coherence and phase-array imaging techniques was employed to locate remaining dominant noise sources. Active control using FxLMS was implemented on the low-frequency noise using a custom hybrid analog/digital reference circuit phase-locked to the generator output. High-frequency passive treatment included panel stiffening and absorbing material. Overall global sound reduction was 15-20dB for tones in the active control bandwidth to 500 Hz. The combination of active and passive treatment provided 6.5 dBA broadband reduction from 0-3000 Hz. The overall perception of the active control effect was very good. Future work will focus on integrating the control speaker, transducers, the controller module and power amplifiers into the generator set enclosure. Consideration will be given to minimizing ANC system space requirements and power consumption.

ACKNOWLEDGEMENTS

We would like to acknowledge the Department of Defense Project Manager for Mobile Electric Power for the funding of this project, awarded under Fibertek subcontract No: 224058-070790. We are also grateful to Jon Carpenter and Wes Moyers of the U.S. Army, CERDEC Power Generation Branch, Ft. Belvoir, VA for very useful technical input and assistance.

REFERENCES

[1.] C. R. Fuller, S. J. Elliott and P. A. Nelson, Active *Control of Vibration* (Academic Press 1996).

[2.] S. M. Kuo and D. R. Morgan, "Active Noise Control: A Tutorial Review," *Proceedings of the IEEE* **87**(6), 943-973 (1999).